Supporting information

Tuning the Threshold Voltage of Carbon Nanotube Transistors by n-Type Molecular Doping for Robust and Flexible Complementary Circuits

Huiliang Wang[1, #], Peng Wei[2, #], Yaoxuan Li[3], Jeff Han[2], Hye Ryoung Lee[3], Benjamin D. Naab[4], Nan Liu[2], Chenggong Wang[5], Eric Adijanto[2], Benjamin C-K. Tee[3], Satoshi Morishita[2], Qiaochu Li[2], Yongli Gao[5], Yi Cui[1], Zhenan Bao[2]

[1] Department of Materials Science and Engineering, [2] Department of Chemical Engineering, [3] Department of Chemical Engineering, [4] Department of Chemistry, Stanford University, California 94305, USA. [5]Department of Physics and Astronomy, University of Rochester, Rochester, NY 14627, USA

[#] These authors contributed equally.

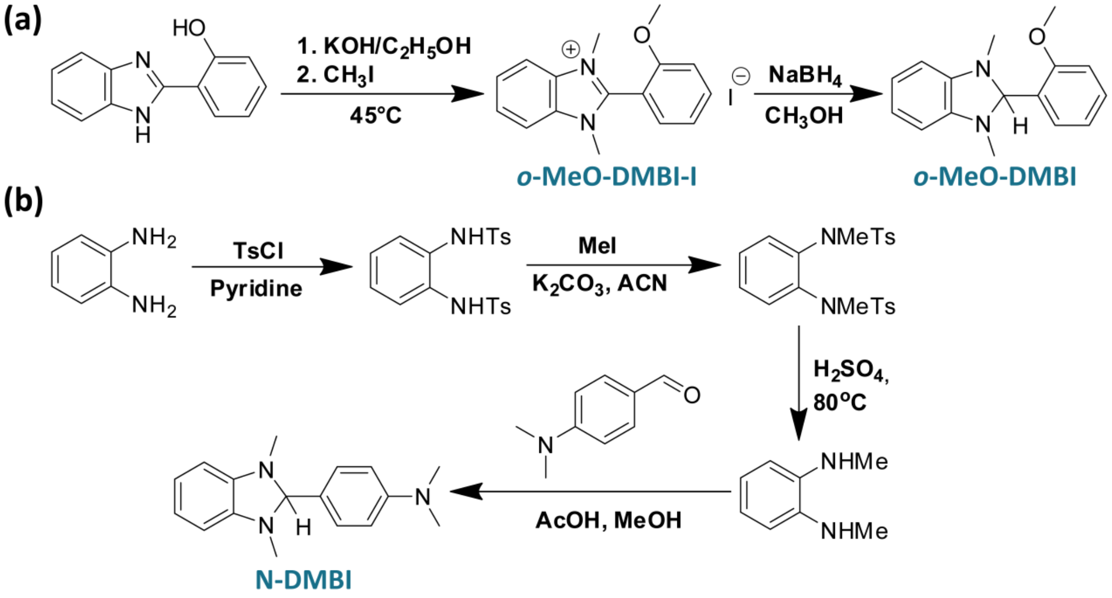

Figure S1. Synthesis schemes for a) o-MeO-DMBI-I, o-MeO-DMBI and b) N-DMBI.

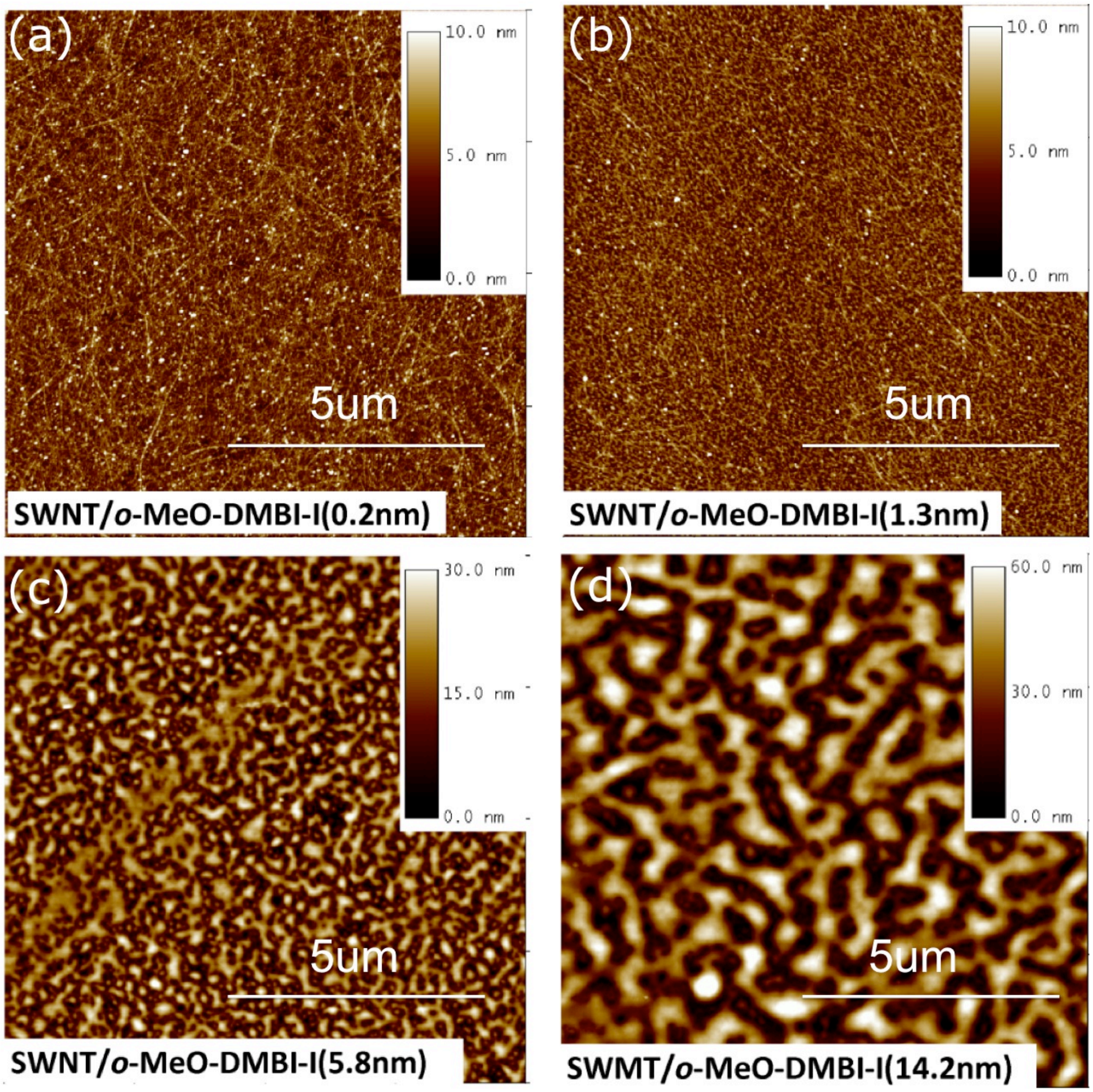

Figure S2. Tapping mode AFM images of SWNT networks with a) 0.2 nm, b) 1.3 nm, c) 5.8 nm, and d) 14.2 nm dopant layer thicknesses, using O-MeO-DMBI-I as the dopant.

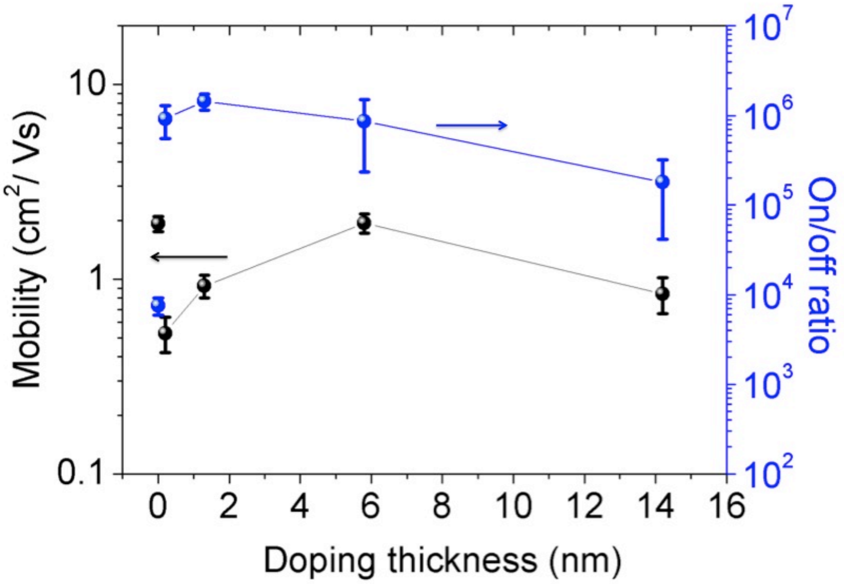

Figure S3. Mobility and on/off ratio of undoped and doped sc-SWNT devices as a functional of the thickness of *o*-MeO-DMBI-I. Five devices were characterized for each doping thickness, with error bars showing the standard deviation from the average value.

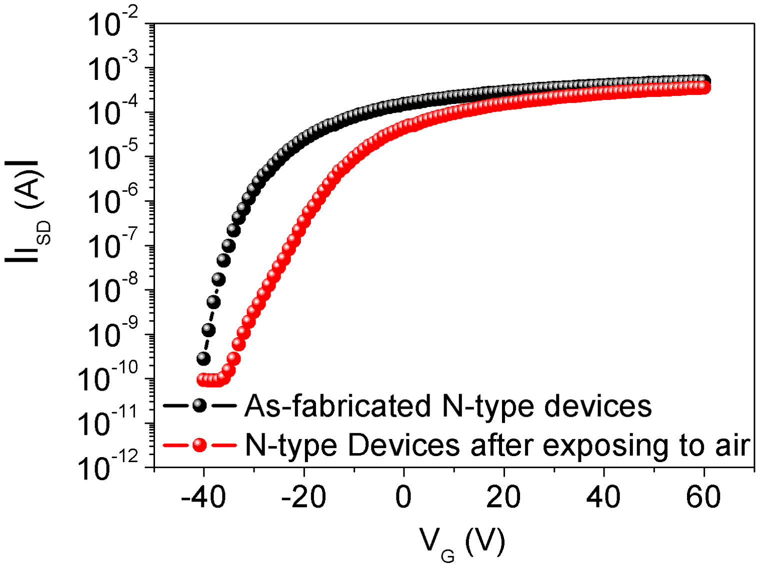

Figure S4. SWNT TFT doped by 3nm *o*-MeO-DMBI-I, measured just after doping (black curve) or after exposing to air for a week (red curve). Both devices were measured under N_2 atmosphere in glovebox.

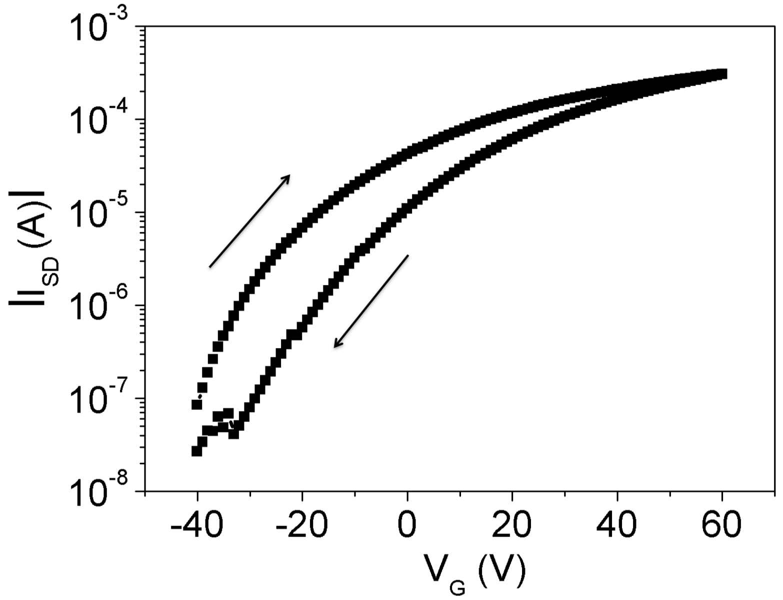

Figure S5. Hysteresis of an n-doped SWNT TFT doped by 3nm *o*-MeO-DMBI-I.

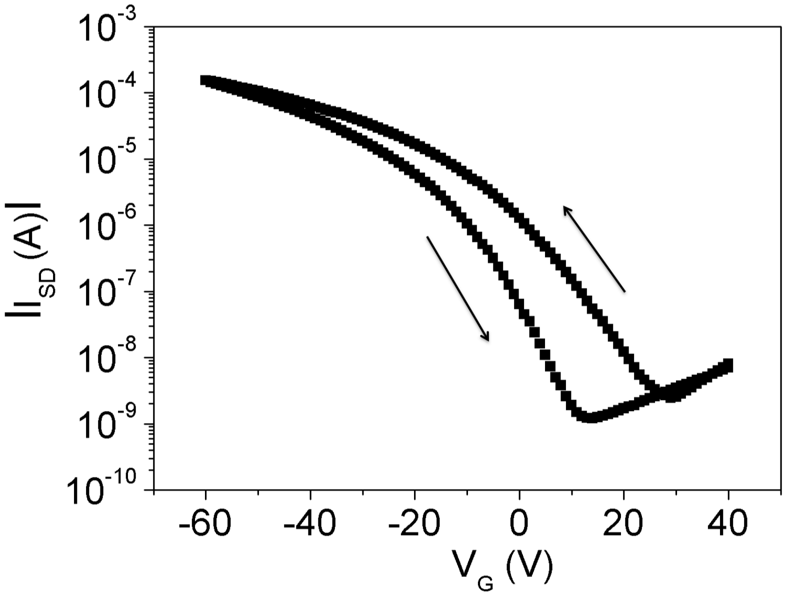

Figure S6. Hysteresis of an un-doped p-type SWNT TFT.

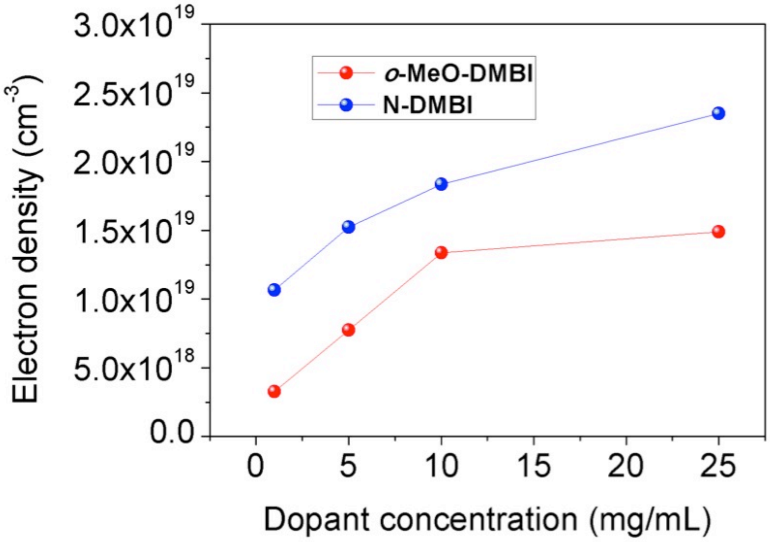

Figure S7. Calculated electron carrier density as a function of *o*-MeO-DMBI and N-DMBI concentrations.

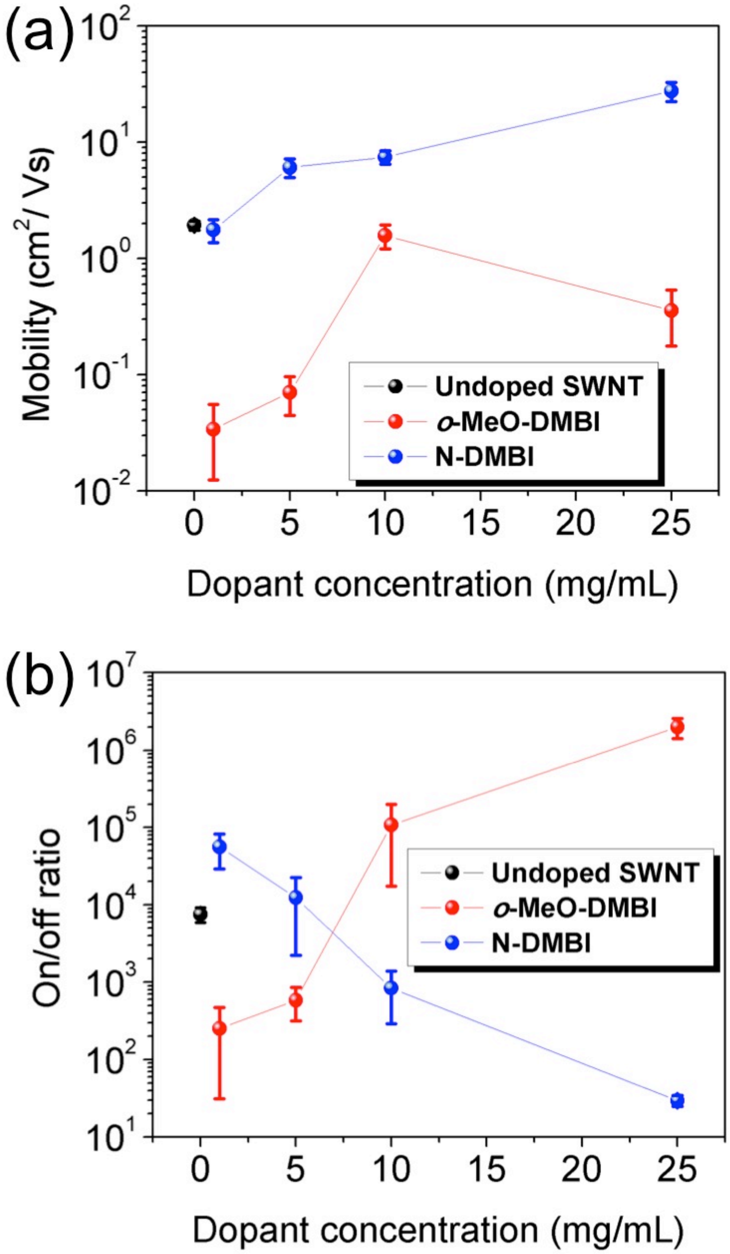

Figure S8. (a) Mobility of the undoped and doped sc-SWNT transistors as a function of *o*-MeO-DMBI and N-DMBI solution concentration. (b) On/off ratio of undoped and doped sc-SWNT transistors as a function of *o*-MeO-DMBI and N-DMBI solution concentration. Five devices were characterized for each doping thickness, with error bars showing the standard deviation from the average value.

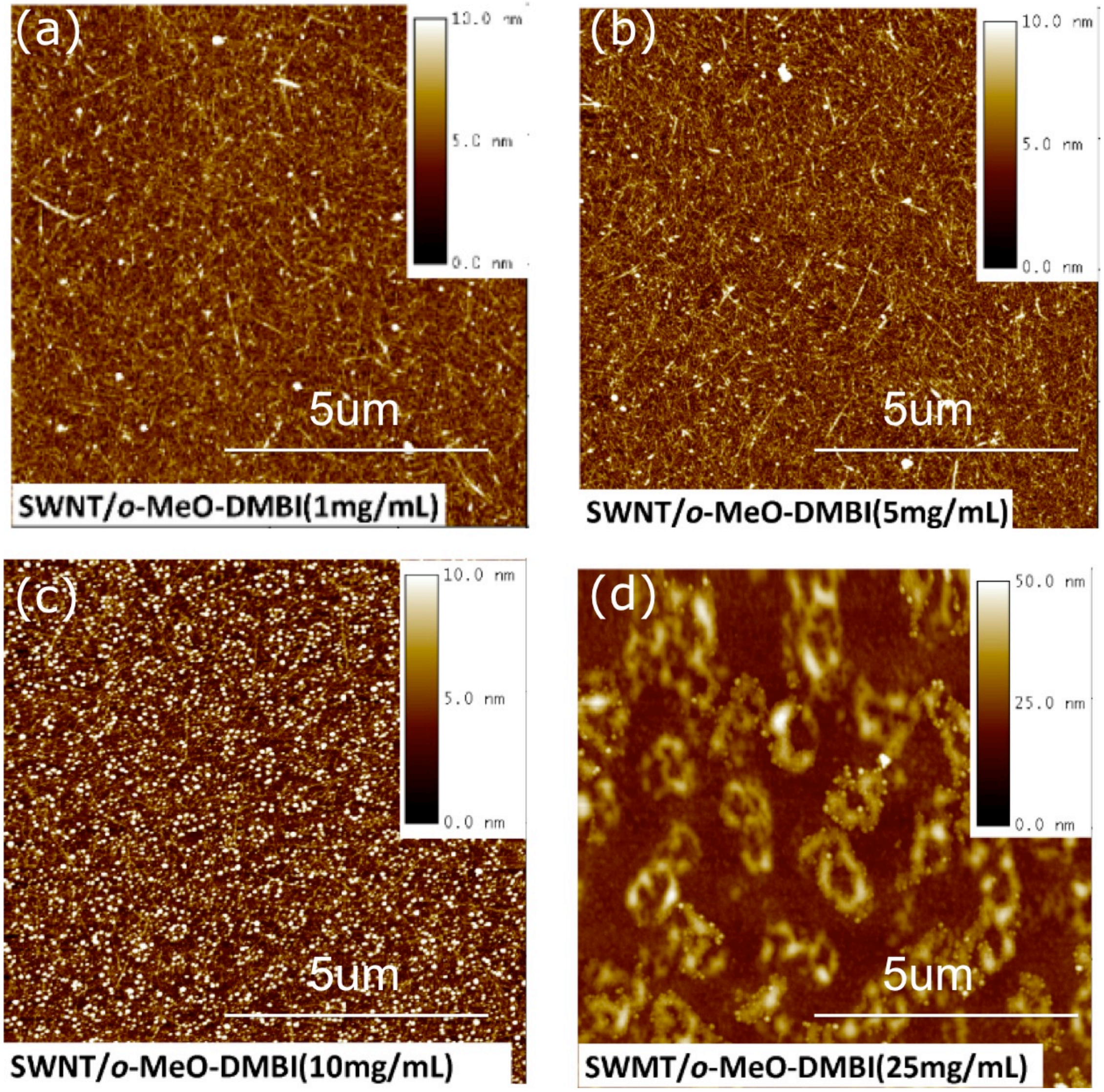

Figure S9. Tapping mode AFM images of SWNT networks doped using a) 1 mg/mL, b) 5 mg/mL, c) 10 mg/mL, and d) 25 mg/mL solutions of *o*-MeO-DMBI.

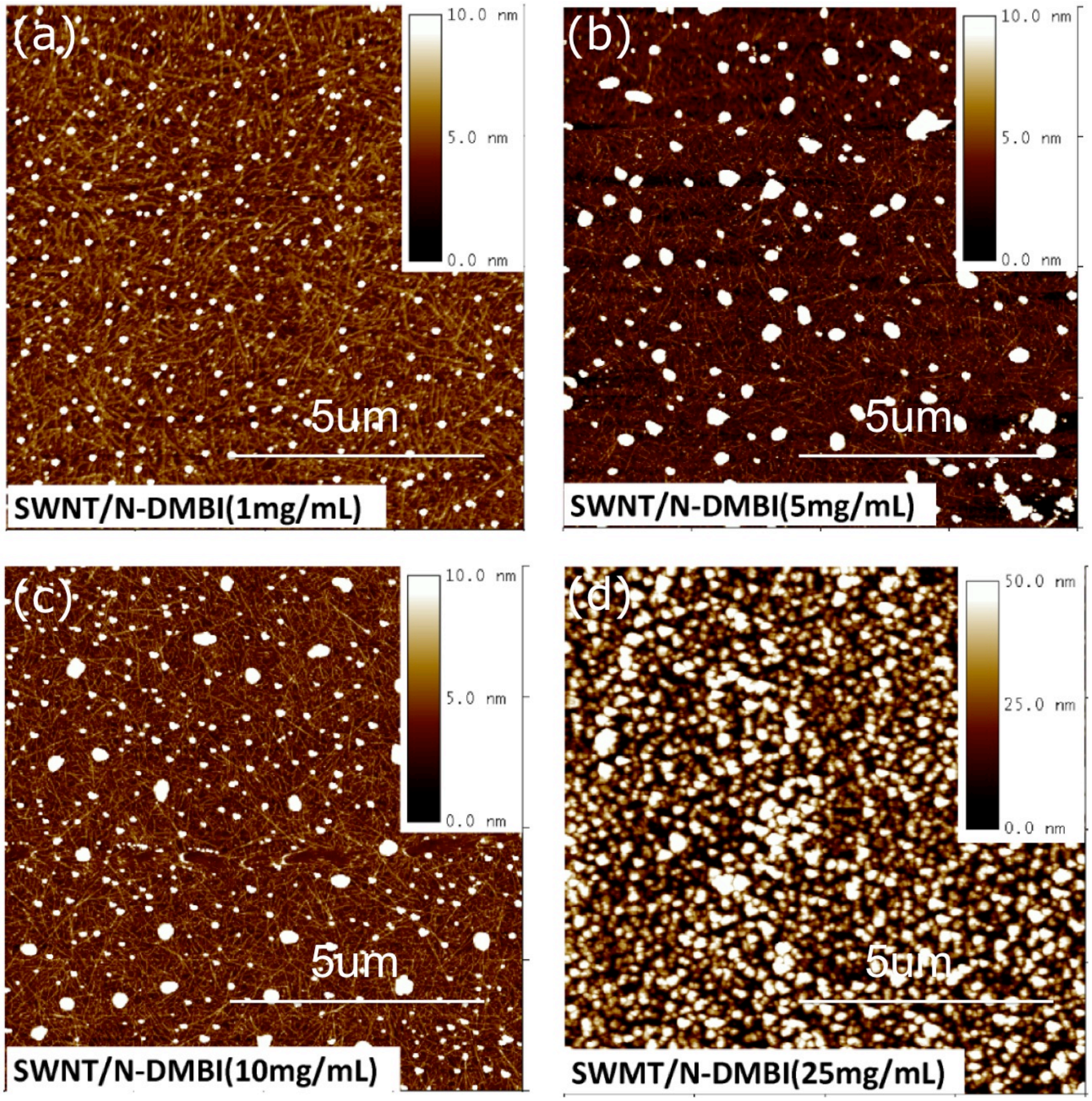

Figure S10. Tapping mode AFM images of SWNT networks doped using a) 1 mg/mL, b) 5 mg/mL, c) 10 mg/mL, and d) 25 mg/mL solutions of N-DMBI.

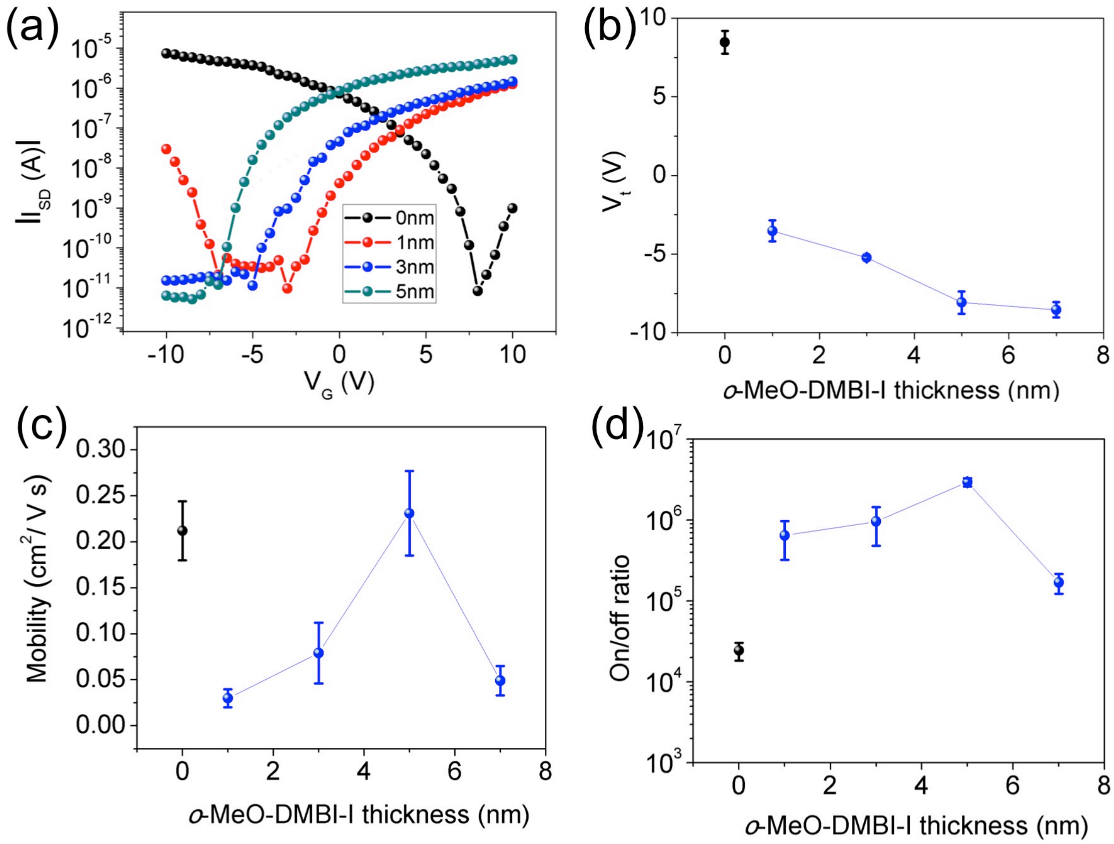

Figure S11. Electrical characteristics of n-type doped flexible transistors (L = 20 µm, W = 400 µm). (a) Transfer characteristics of undoped and doped sc-SWNT transistors as a function of *o*-MeO-DMBI-I layer thickness, V_{SD} = 5 V for n-type and V_{SD} = -5 V for p-type devices. (b) Threshold voltage of undoped and doped sc-SWNT flexible transistors as a function of *o*-MeO-DMBI-I layer thickness. (c) Mobility of the undoped and doped sc-SWNT flexible transistors as a function of *o*-MeO-DMBI-I layer thickness. (d) On/off ratios of the undoped and doped sc-SWNT transistors as a function of *o*-MeO-DMBI-I layer thickness. Five devices were characterized for each doping thickness, with error bars showing the standard deviation from the average value.

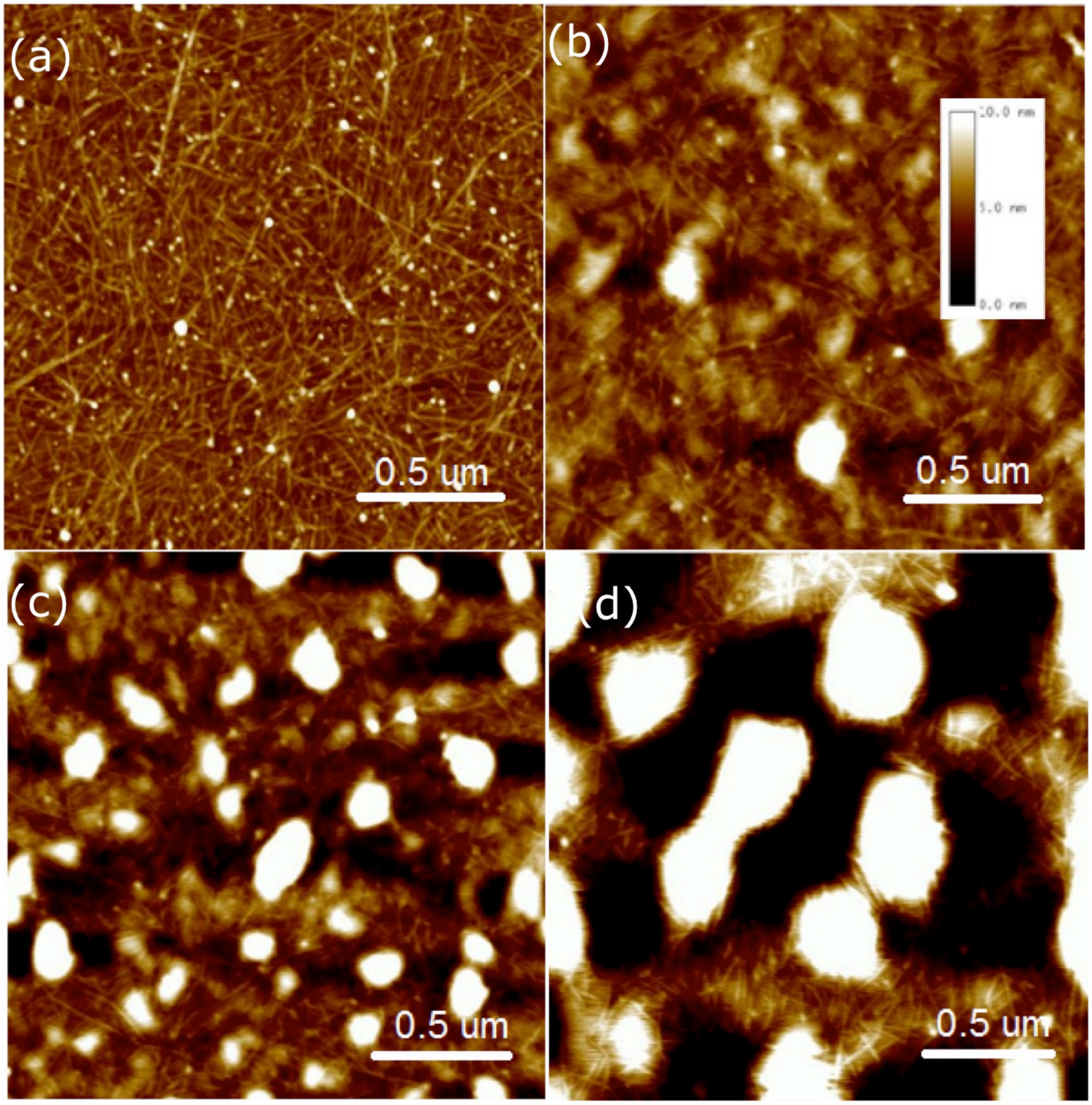

Figure S12. Tapping mode AFM images of SWNT networks on flexible substrate with a) 1 nm, b) 3 nm, c) 5 nm, and d) 7 nm dopant thicknesses of *o*-MeO-DMBI-I.